4454 *Chem. Mater.* **2009,** *21,* 4454–4461
DOI:10.1021/cm9010663

CHEMISTRY OF MATERIALS
Article

A General and Flexible Synthesis of Transition-Metal Polyphosphides via PCl_3 Elimination

Brian M. Barry and Edward G. Gillan*

Department of Chemistry and the Nanoscience and Nanotechnology Institute, University of Iowa, Iowa City, Iowa 52242

Received April 17, 2009. Revised Manuscript Received August 7, 2009

We report a straight-forward, solvent-free moderate temperature synthetic method for the production of several *phosphorus-rich* transition-metal phosphides (orthorhombic FeP_2, cubic CoP_3, cubic NiP_2, monoclinic CuP_2, and monoclinic PdP_2). Notably, this synthetic approach provides facile access to the high-temperature/high-pressure cubic phase of NiP_2. The general synthetic strategy involves the direct reaction of anhydrous metal dichloride pressed pellets with molecular P_4 vapor or solid−solid reactions between the metal dichloride and red phosphorus that are intimately mixed into pellets. Both of these reaction strategies involve the evolution of a volatile PCl_3 byproduct and produce crystalline MP_x ($x \geq 2$) at moderate temperatures of 500−700 °C. The pellets remain intact throughout the synthesis, and the macrostructure of the MP_x products resembles that of the reactant pellets. By varying the phosphorus source, the percentage of the pellet precursor mass that is retained in the final metal phosphide pellet products changes, which influences the morphology and microstructure of the final phosphide pellet.

Introduction

Many solid-state binary phases consisting of a metal and a nonmetal have chemical and physical properties that have found practical applications in recent years. For example, several function as hard ceramics or electrical insulators (WC, ZrO_2, SiO_2),[1,2] or are found in magnetic recording media (CrO_2)[3,4] and in optically emissive or photocatalytic systems (e.g., GaN, TiO_2, CdS, ZnSe).[5−8] While synthetic development trends frequently target the discovery of compositionally complex solid-state structures, simpler binary phases continue to be at the forefront of considerable materials chemistry research, particularly in nanoparticulate bottom-up growth strategies. Materials growth challenges include the search for novel phases and compositions with tunable morphological control that are accessible through improved synthetic methods.

Transition-metal phosphides represent an important class of binary metal/nonmetal compounds with a wide diversity of composition, structure and properties, all of which are, to a large extent, derived from the ability of phosphorus to exist as isolated anions or larger polyphosphide network anions with direct P−P bonding.[9] This flexibility in the phosphide anion structure provides the opportunity to form metal phosphides with varying metal:phosphorus ratios,[10] ranging from metal-rich (MP_x, where $x < 1$) to monophosphide (MP) and phosphorus-rich polyphosphide structures (MP_x, where $x > 1$). Metal-rich metal phosphides have received the greatest attention for their utility as corrosion-resistant materials,[11] catalysts for the hydrodesulfurization of petroleum fuels,[12] and as oxygen barriers in capacitors.[13] Phosphides such as MnP and CoP[14,15] have been investigated for their magnetic properties, FeP has been explored as a potential anode material for lithium-ion batteries,[16] and GaP is a component of green light-emitting diodes (LEDs).[17] Both metal-rich phosphides and monophosphides have been successfully

*Author to whom correspondence should be addressed. E-mail: edward-gillan@uiowa.edu.

(1) Chen, J. G. *Chem. Rev.* **1996**, *96*, 1477–1498.
(2) Chang, J. P.; Lin, Y. S.; Berger, S.; Kepten, A.; Bloom, R.; Levy, S. *J. Vac. Sci. Technol., B* **2001**, *19*, 2137–2143.
(3) Ensling, J.; Gutlich, P.; Klinger, R.; Meisel, W.; Jachow, H.; Schwab, E. *Hyperfine Interact.* **1997**, *111*, 143–150.
(4) Luitjens, S. B.; Rijckaert, A. M. A. *J. Magn. Magn. Mater.* **1999**, *193*, 17–23.
(5) Carvajal, J. J.; Aguilo, M.; Diaz, F.; Rojo, J. C. *Chem. Mater.* **2007**, *19*, 6543–6547.
(6) Linsebigler, A. L.; Lu, G.; Yates, J. T.Jr. *Chem. Rev.* **1995**, *95*, 735–758.
(7) Biju, V.; Itoh, T.; Anas, A.; Sujith, A.; Ishikawa, M. *Anal. Bioanal. Chem.* **2008**, *391*, 2469–2495.
(8) Landi, B. J.; Castro, S. L.; Ruf, H. J.; Evans, C. M.; Bailey, S. G.; Raffaelle, R. P. *Sol. Energy Mater. Sol. Cells* **2005**, *87*, 733–746.
(9) Von Schnering, H. G.; Hoenle, W. *Chem. Rev.* **1988**, *88*, 243–273.
(10) Corbridge, D. E. C. *Phosphorus: An Outline of Its Chemistry, Biochemistry and Technology*; Fourth Edition; Elsevier: New York, 1990.
(11) Liu, J.; Chen, X.; Shao, M.; An, C.; Yu, W.; Qian, Y. *J. Cryst. Growth* **2003**, *252*, 297–301.
(12) Senevirathne, K.; Burns, A. W.; Bussell, M. E.; Brock, S. L. *Adv. Funct. Mater.* **2007**, *17*, 3933–3939.
(13) Stinner, C.; Prins, R.; Weber, T. *J. Catal.* **2001**, *202*, 187–194.
(14) Chiriac, H.; Moga, A.-E.; Urse, M.; Paduraru, I.; Lupu, N. *J. Magn. Magn. Mater.* **2004**, *272−276*, 1678–1680.
(15) Park, J.; Koo, B.; Yoon, K. Y.; Hwang, Y.; Kang, M.; Park, J.-G.; Hyeon, T. *J. Am. Chem. Soc.* **2005**, *127*, 8433–8440.
(16) Boyanov, S.; Bernardi, J.; Gillot, F.; Dupont, L.; Womes, M.; Tarascon, J. M.; Monconduit, L.; Doublet, M. L. *Chem. Mater.* **2006**, *18*, 3531–3538.
(17) Gu, Z.; Parans Paranthaman, M.; Pan, Z. *Cryst. Growth Des.* **2009**, *9*, 525–527.

Published on Web 08/31/2009

synthesized in several ways. They can be obtained as bulk materials from high-temperature elemental reactions, as films by chemical deposition techniques, and also as nanoparticles via molecular solvothermal reactions.[11,15,18−37]

Phosphorus-rich metal phosphides are typically small band gap semiconductors or semimetals[9] and are often diamagnetic.[38−40] Several of these are being examined as potential anode materials for lithium-ion batteries,[41−49] and skutterudite CoP_3 shows promise as a thermoelectric material.[50,51] Phosphorus-rich metal phosphides are described far less frequently in the literature, compared to their metal-rich metal counterparts. This may be due to the challenges associated with the synthesis of these materials, because they are generally less thermally stable than metal-rich phosphides. Their thermal instabilities limit the ability of these phases to be made by simply heating a mixture of the elements at elevated temperatures. The isolation of the single-phase phosphorus-rich metal phosphides can also be problematic as the coincidental formation of the metal-rich counterpart is common.[13,38,52,53]

Selected phosphorus-rich metal phosphides have been synthesized from the elements (powdered metal and red phosphorus) at high temperatures (700−1200 °C), or at moderate temperatures for extended periods of time in tin fluxes (∼550 °C, >10 days).[22,38,54,55] They can also be made by heating the elements in the presence of a chemical transport agent (Cl_2 or I_2) in sealed ampules (∼600−800 °C).[38,55,56] Less conventional methods such as high energy ball-milling and high-pressure anvil syntheses have also been used to produce phosphorus-rich structures.[41,49,57] All of these routes lack morphological and size control and most require a large energy input and long reaction times.

The syntheses of metal phosphides in solvothermal environments using molecular phosphorus precursors typically leads to the metal-rich phases, even with a large excess of phosphorus present, which may be due to hydrolysis or oxidation of phosphorus reagents at elevated temperatures.[12,15,37,53] To our knowledge, there are only three solvent-aided syntheses that produce phosphorus-rich metal phosphides. One converted metal nanoparticles into metal phosphides, using trioctylphosphine as the solvent and as the phosphorus source at 360 −370 °C (Au_2P_3, PdP_2, and PtP_2).[27,53] Another used phosphorus-containing organometallic complexes that were incorporated into silica xerogels and subsequently decomposed at elevated temperatures of 700 °C (PtP_2).[34] The third example is our recent report describing reactions between dissolved molecular yellow/white molecular P_4 and metal chlorides in superheated toluene that produce amorphous products at 275 °C, which crystallize to CoP_3, NiP_2, and CuP_2 upon annealing at 350−500 °C.[58]

When looking at these previous phosphorus-rich metal phosphide syntheses, one notices that the majority of them occur at moderate temperatures (∼300−700 °C). This range seems to offer sufficient thermal energy to crystallize phosphorus-rich structures while avoiding their decomposition to the metal-rich phases. The lower end of this range is near the limit of most solvothermal strategies, and the upper end is fairly modest for conventional solid-state

(18) Xie, Y.; Su, H. L.; Qian, X. F.; Liu, X. M.; Qian, Y. T. *J. Solid State Chem.* **2000**, *149*, 88–91.
(19) Muller, T. K., T.; Labardi, M.; LuxSteiner, M.; Marti, O.; Mlynek, J.; Krausch, G. *J. Vac. Sci. Technol. B* **1996**, *14*, 1296.
(20) Blackman, C. S.; Carmalt, C. J.; O'Neill, S. A.; Parkin, I. P.; Apostolico, L.; Molloy, K. C. *Chem. Mater.* **2004**, *16*, 1120–1125.
(21) Blackman, C. S.; Carmalt, C. J.; O'Neill, S. A.; Parkin, I. P.; Molloy, K. C.; Apostolico, L. *J. Mater. Chem.* **2003**, *13*, 1930–1935.
(22) Kanatzidis, M. G.; Pottgen, R.; Jeitschko, W. *Angew. Chem., Int. Ed.* **2005**, *44*, 6996–7023.
(23) Kaner, R.; Castro, C. A.; Gruska, R. P.; Wold, A. *Mater. Res. Bull.* **1977**, *12*, 1143–1147.
(24) Chen, L.; Luo, T.; Huang, M.; Gu, Y.; Shi, L.; Qian, Y. *Solid State Commun.* **2004**, *132*, 667–671.
(25) Kim, Y. K.; Cho, Y. W. *J. Alloys Compd.* **2005**, *393*, 211–218.
(26) Hou, H.; Yang, Q.; Tan, C.; Ji, G.; Gu, B.; Xie, Y. *Chem. Lett.* **2004**, *33*, 1272–1273.
(27) Henkes, A. E.; Vasquez, Y.; Schaak, R. E. *J. Am. Chem. Soc.* **2007**, *129*, 1896–1897.
(28) Kleinke, H.; Franzen, H. F. *Angew. Chem., Int. Ed.* **1996**, *35*, 1934–1936.
(29) Kher, S. S.; Wells, R. L. *Chem. Mater.* **1994**, *6*, 2056–2062.
(30) Trentler, T. J.; Hickman, K. M.; Goel, S. C.; Viano, A. M.; Gibbons, P. C.; Buhro, W. E. *Science* **1995**, *270*, 1791–1794.
(31) Hector, A. L.; Parkin, I. P. *J. Mater. Chem.* **1994**, *4*, 279–283.
(32) Treece, R. E.; Conklin, J. A.; Kaner, R. B. *Inorg. Chem.* **1994**, *33*, 5701–5707.
(33) Carmalt, C. J.; Morrison, D. E.; Parkin, I. P. *Polyhedron* **2000**, *19*, 829–833.
(34) Lukehart, C. M.; Milne, S. B.; Stock, S. R. *Chem. Mater.* **1998**, *10*, 903–908.
(35) Jarvis, R. F.Jr.; Jacubinas, R. M.; Kaner, R. B. *Inorg. Chem.* **2000**, *39*, 3243–3246.
(36) Brock, S. L.; Perera, S. C.; Stamm, K. L. *Chem.—Eur. J.* **2004**, *10*, 3364–3371.
(37) Gregg, K. A.; Perera, S. C.; Lawes, G.; Shinozaki, S.; Brock, S. L. *Chem. Mater.* **2006**, *18*, 879–886.
(38) Odile, J. P.; Soled, S.; Castro, C. A.; Wold, A. *Inorg. Chem.* **1978**, *17*, 283–286.
(39) Ackermann, J.; Wold, A. *J. Phys. Chem. Solids* **1977**, *38*, 1013–1016.
(40) Shirotani, I.; Takahashi, E.; Mukai, N.; Nozawa, K.; Kinoshita, M.; Yagi, T.; Suzuki, K.; Enoki, T.; Hino, S. *Jpn. J. Appl. Phys.* **1993**, *32*, 294–296.
(41) Zhang, Z.; Yang, J.; Nuli, Y.; Wang, B.; Xu, J. *Solid State Ionics* **2005**, *176*, 693–697.
(42) Wang, K.; Yang, J.; Xie, J.; Wang, B.; Wen, Z. *Electrochem. Commun.* **2003**, *5*, 480–483.
(43) Tirado, J. L. *Mater. Sci. Eng., R.* **2003**, *R40*, 103–136.
(44) Alcantara, R.; Tirado, J. L.; Jumas, J. C.; Monconduit, L.; Olivier-Fourcade, J. *J. Power Sources* **2002**, *109*, 308–312.
(45) Silva, D. C. C.; Crosnier, O.; Ouvrard, G.; Greedan, J.; Safa-Sefat, A.; Nazar, L. F. *Electrochem. Solid-State Lett.* **2003**, *6*, A162–A165.
(46) Pralong, V.; Souza, D. C. S.; Leung, K. T.; Nazar, L. F. *Electrochem. Commun.* **2002**, *4*, 516–520.
(47) Bernardi, J.; Lemoigno, F.; Doublet, M. L. *Solid State Ionics* **2008**, *14*, 197–202.
(48) Gillot, F.; Boyanov, S.; Dupont, L.; Doublet, M. L.; Morcrette, M.; Monconduit, L.; Tarascon, J. M. *Chem. Mater.* **2005**, *17*, 6327–6337.
(49) Park, C.-M.; Sohn, H.-J. *Chem. Mater.* **2008**, *20*, 6319–6324.
(50) Loevvik, O. M.; Prytz, O. *Phys. Rev. B: Condens. Matter* **2004**, *70*, 195119/1–195119/6.
(51) Watcharapasorn, A.; DeMattei, R. C.; Feigelson, R. S.; Caillat, T.; Borshchevsky, A.; Snyder, G. J.; Fleurial, J. P. *J. Appl. Phys.* **1999**, *86*, 6213–6217.
(52) Takacs, L.; Mandal, S. K. *Mater. Sci. Eng., A* **2001**, *A304−306*, 429–433.
(53) Henkes, A. E.; Schaak, R. E. *Chem. Mater.* **2007**, *19*, 4234–4242.
(54) Shatruk, M. M.; Kovnir, K. A.; Shevelkov, A. V.; Popovkin, B. A. *Angew. Chem., Int. Ed.* **2000**, *39*, 2508–2509.
(55) Braun, D. J.; Jeitschko, W. Z. *Anorg. Allg. Chem.* **1978**, *445*, 157–166.
(56) Kloc, C.; Lux-Steiner, M. C.; Keil, M.; Baumann, J. R.; Doell, G.; Bucher, E. *J. Cryst. Growth* **1990**, *106*, 635–642.
(57) Jeitschko, W.; Donohue, P. C. *Acta Crystallogr., Sect. B: Struct. Sci.* **1975**, *B31*, 574–580.
(58) Barry, B. M.; Gillan, E. G. *Chem. Mater.* **2008**, *20*, 2618–2620.

reactions, which may be why phosphorus-rich phases are reported less than their metal-rich counterparts. Improving synthetic accessibility to phosphorus-rich metal phosphide structures increases the likelihood of discovering new applications for this diverse class of materials. In this article, we describe the discovery of a simple, solvent-free, moderate-temperature route to several phosphorus-rich structures (FeP_2, CoP_3, NiP_2, CuP_2, and PdP_2). This synthetic approach involves the direct thermal reaction of pellets of metal dichloride powders with P_4 vapor or the direct reaction of intimately mixed composite pellets containing red phosphorus and the metal chloride powders. It notably uses a compositionally simple and stoichiometric reaction to produce these metal phosphides, including a high-temperature/pressure NiP_2 phase.

Experimental Section

Metal Phosphide Syntheses Using White/Yellow P_4. The metal halides used were anhydrous $FeCl_2$, $CoCl_2$, $NiCl_2$, $CuCl_2$, and $PdCl_2$ (Alfa-Aesar, 99.5%, 99.7%, 98.0%, 98.0%, and 99.9% purity, respectively); the only other reagent used was elemental white/yellow P_4 (Aldrich, stick, yellow phosphorus, 99+% purity, stored in water). Low-level impurities in white P_4 frequently give it a light yellow appearance. These impurities have been ascribed to traces of polymeric red phosphorus that form upon exposure to UV light.[59] All metal halides were dried under dynamic vacuum at 250 °C for a minimum of 4 h to remove any adsorbed water and stored in an argon-filled glovebox prior to use. Schlenk flasks loaded with sticks of yellow P_4 were briefly evacuated (2 min.) and then loaded into the glovebox. Yellow P_4 can sublime at room temperature and low pressures, so care must be taken to avoid its sublimation into vacuum systems.

In each experiment, the metal dichloride was ground with an agate mortar and pestle in an argon-filled glovebox and then pressed into two or three cylindrical pellets (7 mm in diameter and 2−3 mm thick) using a standard KBr die set. The pellets were carefully ejected from the steel collars and weighed. In a typical NiP_2 reaction, a total mass of $NiCl_2$ pellets was targeted as 156 mg (1.2 mmol). Other reactions were typically conducted with ∼1−1.5 mmol of metal halide. The pellets were then loaded into a Pyrex or silica tube that was sealed on one end (outer diameter (OD) = 12 mm, inner diameter (ID) = 9 mm, and length ≈ 30 cm), being careful not to disrupt the pellet integrity, because they were positioned at the closed end of the ampule. Yellow P_4 was prepared by first shaving off any noticeable oxidized surface material with a razor blade and then cutting off an appropriate amount of P_4 from the stick (99 mg or 0.8 mmol P_4 for a NiP_2 experiment, using 1.2 mmol of $NiCl_2$). The MCl_2:P_4 ratios were chosen such that all chloride forms a PCl_3 byproduct and all remaining phosphorus is used to form the metal phosphide (MCl_2:P_4 molar ratios are 3:2 for MP_2 and 3:2.75 for MP_3). The pieces of P_4 were then added to the tube containing the pellets. The open end of the glass tube was fitted with a Cajon connector and a closed Kontes needle valve, removed from the glovebox, and attached to a Schlenk line. The precursor-containing end of the tube was vertically submerged in liquid N_2 and then evacuated to ∼80 mTorr. Liquid N_2 cooling was required to prevent P_4 from subliming away during evacuation and altering the reagent stoichiometry. After a short (∼2 min) evacuation, the tube was sealed to a length of ∼10 cm with a methane−oxygen torch. Light tapping was used to ensure that the pellets at one end of the sealed ampule were not touching each other. This ampule was carefully placed in the center of a horizontal tube furnace and the two ends of the furnace are stuffed with glass wool cloth to prevent heat loss and minimize undesirable temperature gradients across the ampule. The ampule was then heated linearly over 3 h to 500−700 °C and held there for ∼40 h. With the furnace still at its maximum temperature, the empty end of the ampule was carefully moved to the cooler outside opening of the furnace, leaving the pellet-containing end in the furnace. The ampule was left in this state for ∼20 min to allow the PCl_3 byproduct to condense in the cool end of the ampule. The ampule was then cooled to room temperature outside the furnace at an angle such that the pellets and the PCl_3 remain separated. The ampule was then gently scored and cracked open, being careful to avoid the liquid PCl_3 from contacting the pellets. The isolated product pellets were stored in the glovebox.

Metal Phosphide Syntheses Using Red Phosphorus. The metal halides used were the same as described in the previous section; the only other reagent used was red phosphorus (Aldrich, powder, 99% purity). In an argon-filled glovebox, stoichiometric amounts of the metal halide and red phosphorus (the MCl_2:P molar ratio is 3:8 for MP_2 and 3:11 for MP_3) were thoroughly ground together with an agate mortar and pestle. This powder mixture was then pressed into two or three cylindrical pellets (7 mm diameter and 2−3 mm thick), using a standard KBr die set. The pellets were ejected from the steel collars and weighed. In a typical NiP_2 reaction, the total composite pellet mass was targeted as 250 mg, consisting of 153 mg (1.17 mmol) of $NiCl_2$ and 97 mg (3.13 mmol) of red phosphorus. The pellets were then loaded into Pyrex or silica tubes that were sealed on one end (12 mm OD, 9 mm ID, and ∼30 cm in length), being careful not to disrupt the pellet integrity as they were positioned at the closed end of the tube. The tube was then sealed in the same manner described in the previous section, except that no liquid N_2 was required. The evacuated ampule's orientation in the furnace, the PCl_3 separation, and product pellet isolation and storage were all performed in the same manner as that described in the previous section. The heating profiles for the PdP_2, CuP_2, and NiP_2 were also the same as that described in the previous section. To limit metal halide attack on the ampule walls, the higher-temperature CoP_3 and FeP_2 reactions were performed using slower linear heating ramps over 12 h, to 600 °C and 700 °C, respectively, and were held at those temperatures for 40 h.

Safety Notes. Molecular white P_4 is stable when stored under water; however, it is very pyrophoric and burns with a flame immediately upon contact with oxygen/air. *NOTE: Care should be taken to work with this material in small quantities and to carefully clean all experimental equipment of phosphorus residue by oxidizing it with aqueous bleach.* One must also calculate the ideal internal pressure that could be produced from the moles of PCl_3 gas produced in the sealed ampule at the maximum reaction temperature. In this work, calculated gas pressures of < 10 atm did not result in ampule explosions.

Product Characterization. Solution ^{31}P NMR of the liquid byproducts in C_7D_8 was performed on a 400 MHz Bruker DRX-400 system. An external reference sample of H_3PO_4 (δ = 0.0 ppm) was used for calibration. The phase and crystallinity of the products were analyzed by powder X-ray diffraction (XRD), using a Siemens D5000 diffractometer (Cu Kα radiation) for the Cu, Ni, and Pd samples. The Fe and Co samples can absorb Cu

(59) Threlfall, R. E. *The Story of 100 Years of Phosphorus Making, 1851−1951*; Albright and Wilson, Ltd.: Oldbury, U.K., 1951.

Kα X-rays, resulting in low-intensity peaks and an unacceptable fluorescence background, so a Rigaku MiniFlex II diffractometer with a Co Kα radiation souce was used for the Fe and Co samples. The 2θ values for all data are plotted based on Cu Kα radiation, for the sake of consistency. Standard patterns were generated by inputting known crystallographic data into the PowderCell computer program.[60,61] Thermogravimetric−differential thermal analysis (TG-DTA) was performed on a Seiko Exstar 6300 system in alumina pans under an argon flow with a heating rate of 10 °C/min. Very small samples (< 5 mg) were used as gaseous P_4 is generated, which can react with and corrode platinum components of the TGA system. Scanning electron microscopy (SEM) analyses were performed on a Hitachi S-4800 system on pellet shards that had been affixed to aluminum sample stubs with carbon paint. Elemental analyses were performed on a Hitachi S-3400N with EDS capabilities. Bulk elemental analysis of selected samples was performed using inductively coupled plasma−atomic emission spectroscopy (ICP-AES) (Varian Model ICP-OES 720-ES). Samples were first dissolved in hot concentrated HNO_3 and then diluted with deionized (DI) H_2O to 5% HNO_3 by volume.

Results and Discussion

Metal Phosphide Formation via PCl_3 Elimination. In this study, we investigated the direct reaction of metal dichlorides (M = Fe, Co, Ni, Cu, and Pd) with either gaseous molecular yellow P_4 or with solid polymeric red phosphorus in sealed, evacuated glass ampules. In the molecular P_4 reactions, the metal chloride was finely ground and formed into lightly pressed pellets. In the red phosphorus reactions, the metal chloride and the red phosphorus were ground together and pressed into well-mixed composite pellets. In contrast to most prior metal phosphide precursor reactions, the chemical exchange reactions in this research study were *stoichiometrically balanced*, such that all the chlorine was ideally removed as PCl_3 and any remaining phosphorus (yellow P_4 or red phosphorus) formed the metal phosphide product (eq 1).

$$3MCl_2+(2+3x)P \rightarrow 3MP_x+2PCl_3 \quad (1)$$

The evacuated sealed ampules were slowly heated in a tube furnace to maximum temperatures ranging from 500 to 700 °C. Optimal maximum reaction temperatures were determined as the temperature necessary to crystallize the products within ~2 days. For example, CuP_2 and NiP_2 will crystallize at 350 °C; however, durations of 4 days were required for reaction completion (see Table 1 for reaction temperatures). The higher-temperature red phosphorus reactions targeting FeP_2 and CoP_3 at 600 and 700 °C, respectively, required a slower heating ramp (12 h) versus all other experiments (3 h), because ampule etching and silica contamination in the phosphide products was observed when a 3 h ramp was used. The synthesis of FeP_2 and CoP_3 from yellow P_4 did not show evidence of SiO_2 contamination or etching even with the faster heating ramp, likely because of the high reactivity of yellow P_4, compared to red phosphorus. Our working hypothesis is that reactions with red phosphorus are incomplete after a fast 3 h ramp and unreacted metal halide can attack the silica ampule, resulting in SiO_2 contamination in the product pellets. By slowing the heating ramp, the metal halide is given the needed time to completely react with red phosphorus, which prevents its high-temperature reaction with the ampule.

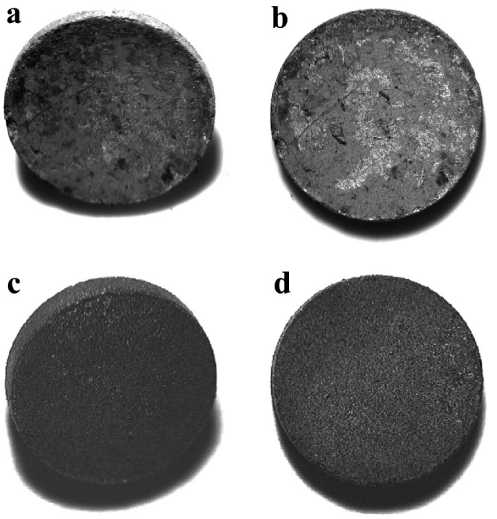

Figure 1. Optical micrographs of MP_x product pellets of (a) CoP_3 synthesized from yellow P_4, (b) NiP_2 synthesized from yellow P_4, (c) PdP_2 synthesized from red phosphorus, and (d) CuP_2 synthesized from red phosphorus. Product pellet diameters from all reactions were 7.0 mm ± 0.5 mm.

In all reactions, the metal chloride or metal chloride/phosphorus composite pellets showed a distinct color change to gray/black by 250 °C, indicating initial phosphorus reaction with the metal halide. When one end of the ampule was pulled out of the 250 °C furnace, a small amount of colorless liquid condensed at the cool end, indicating that PCl_3 formation was beginning. After the reactions were finished, the identity of the clear liquid byproduct was determined to be PCl_3 in all reactions by ^{31}P NMR (δ = 220 ppm). We also detected some $POCl_3$ in all ^{31}P NMR spectra (δ = −2.25 ppm), which is not surprising, because the PCl_3 is briefly in contact with air during its separation from the pellet product.

Pressed reagent pellets were utilized to demonstrate this approach's ability to form microstructured metal phosphide monoliths though vapor infiltration or intimate solid-state reactions between the powdered metal halide and phosphorus reagents. The integrity of the pellets was retained when the metal chloride was converted to its corresponding metal phosphide and the overall size and shape of the pellet was unchanged (~7 mm diameter before and after reaction). Phosphide product pellets from the yellow P_4 reactions appear silver with a metallic luster, with the exception of the yellow P_4 CuP_2 reaction, which produced a slightly expanded pellet with a rough flaky surface. In contrast, the pellets from the red phosphorus reactions appear black and matted (see Figure 1). This difference in pellet appearance is attributed to the increase in voids in the red phosphorus products, because

(60) Villars, P. *Pearson's Handbook of Crystallographic Data for Intermetallic Phases*; ASM International: Materials Park, OH, 1991.
(61) Zachariasen, W. H. *Acta Crystallogr*. **1963**, *16*, 1253–1255.

Table 1. Phosphorus-Rich MP_x Synthesis and Product Analysis

target phase	P source	reaction temperature (°C)	percentage of original mass[a]	MP_x analysis, M:P:Cl[b]	TGA decomposition temperature (°C)[c]
FeP_2	yellow P_4	700	92.0	1:2.00: < 0.01	735 (828)
FeP_2	red phosphorus	700	56.3	1:1.98: < 0.01	750 (849)
CoP_3	yellow P_4	600	117	1:3.06: < 0.01	815 (920)
CoP_3	red phosphorus	600	62.4	1:2.79: < 0.01	780 (876)
NiP_2	yellow P_4	500	95.9	1:2.00:0.01	595 (660)
NiP_2	red phosphorus	500	59.7	1:1.89:0.04	575 (660)
CuP_2	yellow P_4	500	93.3	1:1.96:0.01	555 (647)
CuP_2	red phosphorus	500	57.2	1:1.83:0.03	520 (627)
PdP_2	yellow P_4	500	94.9	1:2.16:0.01	770 (865)
PdP_2	red phosphorus	500	66.1	1:2.17:0.02	760 (874)

[a] Experimental results for (product pellet mass)/(reagent pellet mass) × 100. [b] Molar ratios from EDS data. [c] Data from TG-DTA analysis, decomposition temperature onset (temperature of 10% weight loss).

of a significant loss in pellet mass during the reaction. The pellets from the yellow P_4 reactions forming MP_2 from MCl_2 exchange two Cl atoms (~71 amu) for two P atoms (~62 amu), resulting in a minimal net loss in pellet weight; except in the CoP_3 case, where the product pellet is slightly heavier than the initial $CoCl_2$ pellet. In contrast, the red phosphorus reactions eliminate PCl_3 from the pellets, leading to significantly greater net pellet mass loss than in the corresponding yellow P_4 reactions, because red phosphorus is part of the pellet's initial mass (see Table 1). For example, the ideal CuP_2 pellet's product mass, assuming complete reaction, as a percentage of initial starting pellet mass is 93.3% for a yellow P_4 reaction and only 57.8% for a red phosphorus reaction. The pellet product mass data in Table 1 are consistent with essentially quantitative conversion for each reaction studied (assuming phosphide product pellets), indicating that the ideal proposed reactions based on eq 1 are efficiently occurring in these phosphide syntheses.

Phase Determination and Elemental Analysis. Upon cooling, the pellet-containing ampules were carefully cracked to avoid PCl_3 contact with the final pellets. The pellets were analyzed with no further processing or workup to avoid potential surface reactions. Powder XRD patterns of ground pellets were taken to determine the crystalline phases contained in each product pellet (see Figure 2 and Figure S1 in the Supporting Information). The patterns revealed the presence of the crystalline phosphides corresponding to compositions targeted in eq 1 for both the yellow P_4 and red phosphorus reactions: specifically, orthorhombic FeP_2,[60] cubic CoP_3,[60] cubic NiP_2,[60] monoclinic CuP_2,[60] and monoclinic PdP_2.[61] The cubic NiP_2 phase was obtained in both the yellow P_4 and red phosphorus reactions, which is unexpected, because this structure is not commonly observed and has previously been described as a high-temperature, high-pressure phase (1200 °C, 6.5 GPa).[62] The ambient pressure form of NiP_2 is the monoclinic structure, which is closely related to the PdP_2 phase observed in this work.[63]

Energy-dispersive spectroscopy (EDS) analysis of the isolated metal phosphides revealed that the products had M:P molar ratios near their expected 1:2 or 1:3 values and little or no detectable chlorine residue (see Table 1). Products from yellow P_4 reactions targeting copper, nickel, and cobalt phosphides have slightly higher phosphorus contents than their red phosphorus counterparts, which may indicate more-efficient phosphorus incorporation using yellow P_4 in these reactions. Bulk ICP-AES elemental analysis of the CuP_2 and NiP_2 from

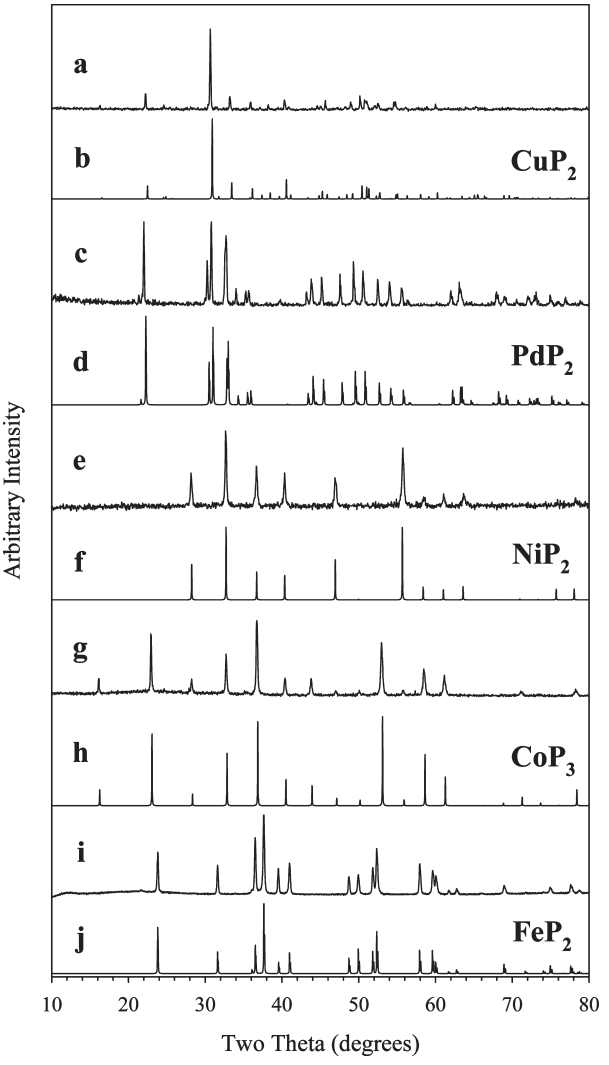

Figure 2. Experimental XRD patterns for MP_x products from yellow P_4 reactions: monoclinic CuP_2 (pattern a), monoclinic PdP_2 (pattern c), cubic NiP_2 (pattern e), cubic CoP_3 (pattern g), and orthorhombic FeP_2 (pattern i). The patterns just below each of the experimental patterns (patterns b, d, f, h, and j) are the calculated patterns for the respective phase.

(62) Donohue, P. C.; Bither, T. A.; Young, H. S. *Inorg. Chem.* **1968**, *7*, 998–1001.
(63) Rundqvist, S. *Acta Chem. Scand.* **1961**, *15*, 451–453.

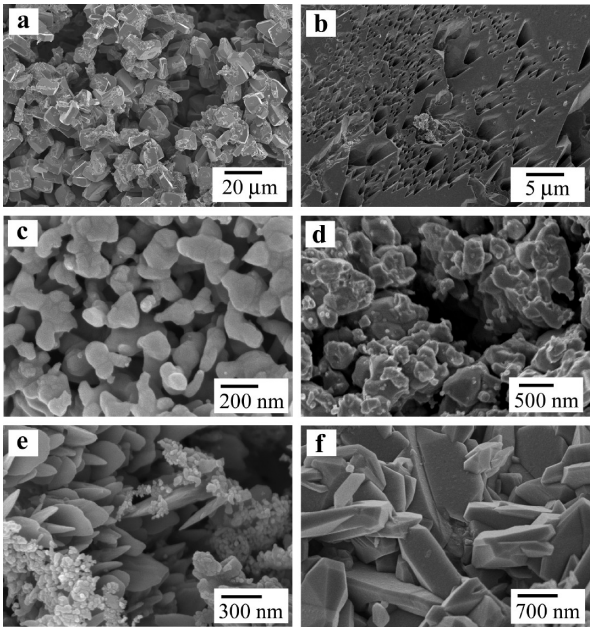

Figure 3. SEM images of (a) CuP_2 synthesized from red phosphorus, (b) CuP_2 synthesized from yellow P_4, (c) NiP_2 synthesized from red phosphorus, (d) NiP_2 synthesized from yellow P_4, (e) PdP_2 synthesized from red phosphorus, and (f) FeP_2 synthesized from yellow P_4.

reactions with red phosphorus confirmed the EDS M:P molar ratio results.[64]

Phosphide Pellet Morphologies. Each phosphide pellet from the syntheses outlined in Table 1 has distinct morphological features, as determined by scanning electron microscopy (SEM). For example, the CuP_2 product from the red phosphorus reaction is comprised of similarly shaped, fused, faceted polyhedra that range in size from 10 μm to 20 μm along their longest edge (see Figure 3a and Figure S2 in the Supporting Information). The CuP_2 product from the yellow P_4 reaction consists of large faceted domains (> 50 μm) that contain sharp crags and pinholes scattered on their surface (see Figure 3b and Figure S2 in the Supporting Information). The yellow P_4 product seems to have less void space than CuP_2 from red phosphorus, which is consistent with the earlier discussion of pellet mass loss being larger for the red phosphorus composite reagent pellets. The NiP_2 products from red phosphorus and yellow P_4 reactions both consist of fused masses of irregular particles with smooth surfaces and features ranging from 50 nm to 200 nm for the red phosphorus product to larger 100−600 nm sizes for the yellow P_4 product (see Figures 3c and 3d and Figure S2 in the Supporting Information). The PdP_2 pellet synthesized from red phosphorus shows fused clusters of spherical particles, in the size range of ~20−300 nm, along with thin plates (~30 nm in thickness and ~500 nm in diameter) that seem to be growing from the fused spherical particles (see Figure 3e and Figure S2 in the Supporting Information). The FeP_2 products from both the yellow and red phosphorus reactions contained fused, faceted large crystallites with a variety of shapes and sizes

(64) ICP-AES data: M:P molar ratio (M wt %, P wt %). NiP_2 − 1:2.020 (44.9, 47.9); CuP_2 − 1:1.848 (52.0, 46.8).

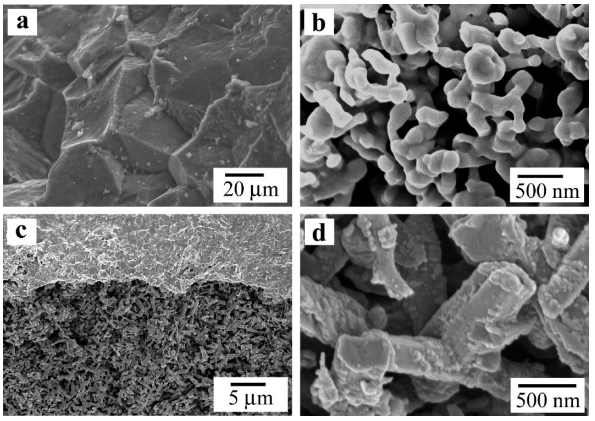

Figure 4. SEM images of (a) CoP_3 synthesized from yellow P_4 at 600 °C for 2 d, (b) CoP_3 synthesized from red phosphorus at 600 °C for 2 d, and (c, d) CoP_3 synthesized from yellow P_4 at 500 °C for 1 d.

(submicrometer to ~5 μm; see Figure 3f and Figure S2 in the Supporting Information).

The CoP_3 product from yellow P_4 is different from the other reactions in that the pellet gains weight during the reaction, which leads to a pellet with no visible voids (see Figure 4a) and smooth fused surface features at higher magnification (see Figure S2 in the Supporting Information). In contrast, the CoP_3 product from red phosphorus has smooth fused particle-like features ranging from 150 to 500 nm in size (see Figure 4b and Figure S2 in the Supporting Information). When the CoP_3 reaction with yellow P_4 was performed at a lower temperature (500 °C) and held for only one day, as opposed to two days, the product is morphologically different. This CoP_3 product pellet, which consists of poorly crystalline CoP_3 by XRD analysis, has a clear morphological contrast between the pellet crust and its interior (see Figures 4c and 4d). Under a continuous surface, there are numerous fused rod-shaped particles (~400 nm in diameter, 2 μm in length). When these pellets are heated at 600 °C for an additional day, they convert to a nonporous, solid mass similar to that shown in Figure 4a.

Although control of pellet porosity was not targeted in this study, even the visibly porous pellets seem to have interconnected structures. As a qualitative test, all phosphide pellets register a measurable two-probe resistance value across the pellet surface (~10 Ω to 300 Ω), indicating the presence of conducting pathways. The exceptions were the CuP_2 samples that showed higher ~20−80 kΩ values. This is not surprising because CuP_2 has a semiconducting band gap (E_g = 1.5 eV)[65] that is twice that of any of the other phosphides in this study.[40,66−68]

Metal Phosphide Thermal Stabilities. The thermal stability of each phosphide product was studied by thermogravimetric−differential thermal analysis (TG-DTA).

(65) Ugai, Y. A.; Pshestanchick, V. R.; Anokhin, V. Z.; Gukov, O. Y. *Neorg. Mater.* **1974**, *10*, 405–408.
(66) Boda, G.; Stenstrom, B.; Sagredo, V.; Beckman, O.; Carlsson, B.; Rundqvist, S. *Phys. Scr.* **1971**, *4*, 132–134.
(67) Burdett, J. K.; Coddens, B. A. *Inorg. Chem.* **1988**, *27*, 418–421.
(68) Watcharapasorn, A.; DeMattei, R. C.; Feigelson, R. S.; Caillat, T.; Borshchevsky, A.; Snyder, G. J.; Fleurial, J. P. *J. Appl. Phys.* **1999**, *86*, 6213–6217.

The samples were heated to 1000 °C under an argon flow, and their decomposition temperatures are listed in Table 1 as estimated weight loss onset and 10% weight loss temperatures (see Figure S3 in the Supporting Information). All sample weights after TG-DTA decomposition were greater than those expected if the samples decomposed to the metallic elements, which suggests that the remaining products were metal-rich phosphides. When feasible, the TG-DTA residue was analyzed by XRD. XRD data showed that FeP_2 and CoP_3 decomposed to FeP and CoP, respectively, with theoretical weight losses for these transformations that were in good agreement with the experimental results (26.3% and 40.8% for FeP_2 and CoP_3).

Because TG-DTA utilizes an argon flow and our synthetic conditions include a static vacuum, an experiment was conducted to determine if the phosphorus-rich pellets decompose in evacuated ampules at temperatures similar to those of the TG-DTA results. Pellets of CuP_2 and NiP_2 from red phosphorus were resealed in evacuated silica ampules (similar size and furnace orientation as described for phosphide synthesis) and heated to 600 and 650 °C, respectively, for ~15 h. After heating, one end of the tube was pulled out of the furnace, to transport any evolved white P_4 away from the pellets. The resulting pellets were crystalline Cu_3P and Ni_2P by XRD (see Figure S4 in the Supporting Information), confirming that the polyphosphide decomposition temperatures are consistent with TG-DTA results. Overall, the thermal decomposition data shows that phosphorus-rich metal phosphide phases require relatively low synthetic conditions (< 600 °C in some cases) as higher reaction temperatures will lead to their decomposition to metal-rich phosphide phases. Previous elemental synthesis approaches to CuP_2 have shown that excess phosphorus vapor is necessary in order to heat such systems to above 900 °C where CuP_2 melts; otherwise, Cu_3P forms.[69,70] Systems using excess phosphorus may produce pyrophoric molecular white phosphorus byproducts that require more careful handling than the PCl_3 byproducts in the current strategy.

Phosphorus Reactions and Product Formation. As this study shows, crystalline phosphorus-rich metal phosphides are easily synthesized via direct reaction of metal chloride pellets with elemental phosphorus (molecular P_4 vapor or intimate contact with polymeric red phosphorus) resulting in volatile PCl_3 elimination. Figure 5 is a cartoon schematic diagram of the reaction/elimination processes that likely occur during these elemental phosphorus to phosphide transformations. Given the significant mass changes that occur in the red phosphorus reagent pellet during the reaction, more open porous structures generally result. An inert, removable template additive may be a useful tool for converting these phosphide pellets to higher-surface-area, porous phosphide structures or composites. While pressed pellets were used

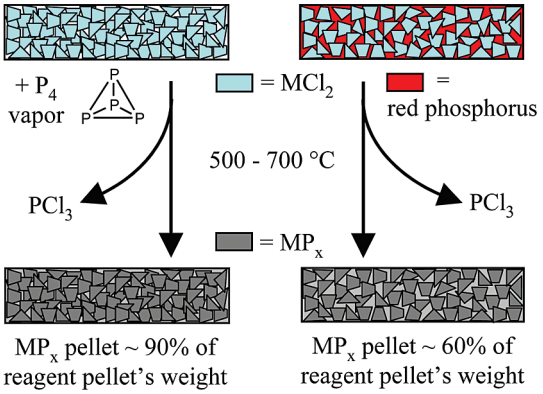

Figure 5. Schematic diagram of MCl_2 pressed pellet reactions with either molecular P_4 vapor or intimate solid-state mixtures with polymeric red phosphorus. The product forms emphasize the overall macrosopic shape retention and relative weight loss during PCl_3 byproduct elimination.

in this study, their use with volatile molecular yellow phosphorus is not required for this synthetic method. This is demonstrated by reactions with lightly ground $CuCl_2$ and $NiCl_2$ powders with yellow P_4 that produced crystalline CuP_2 and NiP_2 under the same heating conditions used for the pellet reactions (see Figure S5 in the Supporting Information). The CuP_2 powder product has a faceted particle microstructure that is similar that observed for pellet products, whereas the NiP_2 product has a distinct crystal shard appearance with fused particles evident upon higher magnification (see Figure S6 in the Supporting Information).

As was discussed earlier, many metal phosphide syntheses produce metal-rich phases or mixtures of phases, even when phosphorus-rich metal phosphides are targeted by reaction stoichiometry. In our reaction system, phosphorus-rich phases are very accessible and even seem to be favored over metal-rich MP_x formation. For example, Co_2P or Cu_3P were targeted using the modifications in reagent stoichiometry according to eq 1 and the same experimental conditions as described previously for the phosphorus-rich metal phosphides. The isolated crystalline products in these Co_2P and Cu_3P syntheses were CoP_3 with significant unreacted $CoCl_2$ and CuP_2 with reduced CuCl, respectively. These results were surprising, because both crystalline metal-rich phases have been previously synthesized at low temperatures (~140 °C).[18]

An examination of reaction thermochemistry for the Co−P and Cu−P systems shows that the formation of phosphorus-rich phases is thermodynamically favored over their metal-rich counterparts in our reactions. The calculated ΔH_{rxn}(298 K) for the cobalt and copper phosphide formation reactions (eq 1), based on the moles of metal in the final product, were determined to be exothermic for CoP_3 (−109 kJ/mol) and CuP_2 (−86 kJ/mol) versus being comparably less exothermic (or endothermic) for Co_2P (+6.7 kJ/mol) and Cu_3P (−35 kJ/mol). In both cases, reaction enthalpy favors the formation of phosphorus-rich phases over their metal-rich counterparts. Note that these calculated enthalpies are room-temperature values that ignore additional entropy energy changes at higher temperatures, primarily because of gaseous PCl_3 vapor production.

(69) Olofsson, O. *Acta Chem. Scand.* **1965**, *19*, 229–241.
(70) Olofsson, O. *Acta Chem. Scand.* **1972**, *26*, 2777–2787.

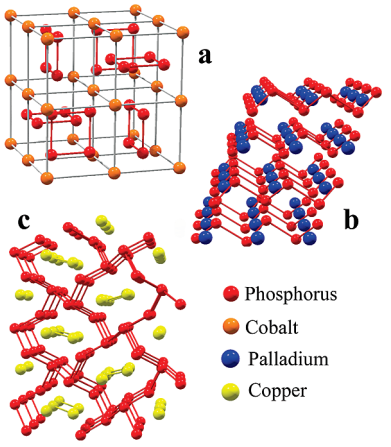

Figure 6. Structural representations of (a) CoP_3 with discrete P_4 rings, (b) PdP_2 with infinite one-dimensional (1D) chains, and (c) CuP_2 with infinite two-dimensional (2D) sheets of fused P_{10} rings.

The use of elemental phosphorus sources with preformed P−P bonds may also play an important role in facilitating the formation of polyphosphide anions in these syntheses. Several structural examples that emphasize P−P networks produced in this study are shown in Figure 6. In contrast, using yellow P_4 or red phosphorus to form metal-rich phases requires the breaking of several reagent P−P bonds to afford small phosphide anions. Thermochemical reaction preferences and P−P precursor bonding effects may also play a role in explaining why reactions with excess alkylphosphine (PR_3, P−R bond breaking required) most readily produce metal-rich phosphides over their phosphorus-rich counterparts.

Conclusions

The reaction of transition-metal dichlorides (M = Fe, Co, Ni, Cu, and Pd) with either yellow P_4 vapor or with intimately mixed red phosphorus in the solid state at temperatures ranging from 500 to 700 °C leads to the formation of crystalline phosphorus-rich MP_x ($x = 2, 3$) phases. In the case of nickel, a high-temperature/high-pressure cubic NiP_2 phase is formed at moderate temperatures. This phosphorus-rich phosphide formation reaction is facilitated by thermochemically favorable processes that include the elimination of a PCl_3 byproduct. The solid powdered reagents were pressed into pellets and retained their macroscopic shape after reaction. The pellet morphologies generally consist of fused particles with smooth to faceted shapes ranging from nanometer to micrometer dimensions. This method represents a rare moderate temperature and stoichiometric synthetic approach to phosphorus-rich metal phosphides.

Acknowledgment. The authors gratefully thank the National Science Foundation (CHE-0407753) for funding this work and Miller Li for performing the ICP-AES analysis.

Supporting Information Available: XRD patterns of red phosphorus reaction products, additional SEM images of pellet reaction products at various magnifications, thermogravimetric analysis data, XRD data for annealed CuP_2 and NiP_2 pellets, and XRD/SEM data for NiP_2 and CuP_2 powder reaction products. This information is available free of charge via the Internet at http://pubs.acs.org.